Heliyon 10 (2024) e30881

Contents lists available at ScienceDirect

Heliyon

journal homepage: www.cell.com/heliyon

Research article

Deep learning system for screening AIDS-related cytomegalovirus retinitis with ultra-wide-field fundus images

Kuifang Du [a,1], Li Dong [b,1], Kai Zhang [c,1], Meilin Guan [a], Chao Chen [a], Lianyong Xie [a], Wenjun Kong [a], Heyan Li [b], Ruiheng Zhang [b], Wenda Zhou [b], Haotian Wu [b], Hongwei Dong [a,**], Wenbin Wei [b,*]

[a] Department of Ophthalmology, Beijing Youan Hospital, Capital Medical University, Beijing, China
[b] Beijing Tongren Eye Centre, Beijing Key Laboratory of Intraocular Tumour Diagnosis and Treatment, Beijing Ophthalmology & Visual Sciences Key Lab, Medical Artificial Intelligence Research and Verification Key Laboratory of the Ministry of Industry and Information Technology, Beijing Tongren Hospital, Capital Medical University, Beijing, China
[c] Chongqing Chang'an Industrial Group Co. Ltd, Chongqing, China

ARTICLE INFO

Keywords:
AIDS
Cytomegalovirus retinitis
deep learning
Ultra-wide-field image
Heat maps

ABSTRACT

Background: Ophthalmological screening for cytomegalovirus retinitis (CMVR) for HIV/AIDS patients is important to prevent lifelong blindness. Previous studies have shown good properties of automated CMVR screening using digital fundus images. However, the application of a deep learning (DL) system to CMVR with ultra-wide-field (UWF) fundus images has not been studied, and the feasibility and efficiency of this method are uncertain.

Methods: In this study, we developed, internally validated, externally validated, and prospectively validated a DL system to detect AIDS-related from UWF fundus images from different clinical datasets. We independently used the InceptionResnetV2 network to develop and internally validate a DL system for identifying active CMVR, inactive CMVR, and non-CMVR in 6960 UWF fundus images from 862 AIDS patients and validated the system in a prospective and an external validation data set using the area under the curve (AUC), accuracy, sensitivity, and specificity. A heat map identified the most important area (lesions) used by the DL system for differentiating CMVR.

Results: The DL system showed AUCs of 0.945 (95 % confidence interval [CI]: 0.929, 0.962), 0.964 (95 % CI: 0.870, 0.999) and 0.968 (95 % CI: 0.860, 1.000) for detecting active CMVR from non-CMVR and 0.923 (95 % CI: 0.908, 0.938), 0.902 (0.857, 0.948) and 0.884 (0.851, 0.917) for detecting active CMVR from non-CMVR in the internal cross-validation, external validation, and prospective validation, respectively. Deep learning performed promisingly in screening CMVR. It also showed the ability to differentiate active CMVR from non-CMVR and inactive CMVR as well as to identify active CMVR and inactive CMVR from non-CMVR (all AUCs in the three independent data sets >0.900). The heat maps successfully highlighted lesion locations.

Abbreviations: AIDS, Acquired immune deficiency syndrome; ROC, Receiver Operating Characteristic; AUROC, Area under the ROC curve; CMVR, Cytomegaloviral retinitis; CI, Confidence interval; DL, Deep learning; DNA, Deoxyribonucleic acid; HIV, Human immunodeficiency virus; UWF, Ultra-wide-field; SD, Standard deviation.

* Corresponding author. Beijing Tongren Hospital, Dong Jiao Min Xiang, Dong Cheng District, 100730 Beijing, China.
** Corresponding author. Beijing You'an Hospital, No.8, Xi Tou Tiao, Youanmen wai, Fengtai District, 100069, Beijing, China.
E-mail addresses: hongweiyanke@163.com (H. Dong), weiwenbintr@163.com (W. Wei).
[1] These authors contributed equally to this manuscript.

https://doi.org/10.1016/j.heliyon.2024.e30881
Received 3 December 2023; Received in revised form 3 May 2024; Accepted 7 May 2024
Available online 15 May 2024

Conclusions: Our UWF fundus image-based DL system showed reliable performance for screening AIDS-related CMVR showing its potential for screening CMVR in HIV/AIDS patients, especially in the absence of ophthalmic resources.

1. Introduction

Cytomegalovirus retinitis (CMVR) is a type of severe, blindness-causing ocular disease that occurs among immunosuppressed groups, especially patients with acquired immune deficiency syndrome (AIDS) [1]. In China, the upsurge of HIV/AIDS cases among college students has aroused great concern from the Chinese government [2]. Young patients can experience restored health via successful antiretroviral therapy, but undiagnosed or inadequately treated CMVR can lead to permanent blindness [3]. Since the last century, an increasing number of experts have promoted regular ophthalmological screening for CMVR in patients with HIV/AIDS to curb visual impairment [4–7].

Traditionally, CMVR diagnosis or screening was conducted by trained ophthalmologists for the dilated examination of the entire retina with an indirect ophthalmoscopy [4]. However, we are facing challenges in terms of structural obstacles, such as the imbalanced distribution of medical resources in different venues [8]. Some HIV/AIDS specialized hospitals in China do not have an ophthalmology department nor the resources to implement ophthalmological screening. Only after they are discharged from local hospitals, patients might obtain a delayed diagnosis and treatment of CMVR at a higher-level hospital. Whereafter, telemedicine screening of CMVR by ophthalmologists or nonophthalmologists using digital fundus photography or UWF fundus image emerged [9–12]. Telemedicine screening provided obvious improvement by saving labor and facilitating remote diagnosis. However it is still limited to labor costs. Besides, some cases still need blood tests or chamber paracentesis for aqueous humor tests, which are invasive and costly [13,14].

Artificial intelligence (AI), represented by deep learning (DL), has incorporated image-processing tasks into everyday clinical practice, thus filling the need for relatively rapid interpretation of images and the lack of local expertise [15,16]. The combination of a DL system and digital fundus photographs, slit-lamp images, or oct has shown potential applications towards the automated detection of various ocular diseases, including diabetic retinopathy, glaucoma, age-related macular degeneration, optic disc diseases, lattice

Table 1
Previous relevant study analysis.

Reference	Disease type (s)	Modality	Dataset size	Sample size	AI problem	Algorithm	Model	Best performance
Shah et al. (2013) [10]	CMVR in HIV patients	Nine-field fundus photographs using a digital fundus camera	370 images	188 HIV patients	Classification	Telemedicine screening**by retina specialists**	–	Sensitivity:30.2 %, Specificity: 99.9 % Kappa values: 0.739 to 0.987
Jirawison et al. (2015) [11]	CMVR in HIV patients	Mosaic fundus photographs using a digital fundus camera	272 images	103 HIV patients	Classification	Telemedicine screenng by retina specialists	–	Sensitivity: 302 %, Specificity: 99.1 %
Yen et al. (2014) [9]	CMVR in HIV patients	Mosaic fundus photographs using a digital fundus camera	182 images	94 HIV patients	Classification	Telemedicine screning by nonophthalmologists	–	Sensitivity: 4.1 %, Specificity:82.3 %, Cohen κ: 0.83
Du et al. (2020) [12]	CMVR in HIV patients	Ultra-wide-field imaging	186 images	94 HIV patients	Classification	Telemedicine sreening by retina specialists	–	Sensitivity: 96.3 %, Specificiy: 100 %, Kappa value: 0.978
ingkosol et al. (2020) [28]	CMVR in imunodefi-cient patients	Fundus photographs using a digital fundus camera	1112 images	249 eyes	Classification	ANN	AWPT-based ANN.	Sensitivty: 90.32 %, Specifiity: 95.71 %, AUC: 95.80 %
Srisuriyajan et al. (2022) [29]	CMVR in HIV patients	A single central field of the fundus photographs using a digital fundus camera	165 images	90 HIV patients	Classification	CNNs	Keras application (VGG16)	Sensiivity: 68.8 %, Speificity: 100 %, Accuracy: 93.94 %
Ong et al. (2024) [13]	NIU-PS, ARN, and CMVR	Blood and serology test	156 CMVR	156 CMVR	Classification	DNNs	MTL	ROC-AUC: 0.982, PRC-AUC:0.807

ANN = artificial neural network; ARN = acute retinal necrosis; AWPT = adaptive wavelet packet transform; NIU-PS = noninfectious uveitis of the posterior segment; DNNs = deep neural networks; CNNs = convolutional neural networks; MTL = multi-task learning; PRC-AUC = precision recall curve-area under the curve; ROC-AUC = receiver operating characteristic curve-area under the curve.

degeneration, and retinal breaks [17–25]. Automated CMVR screening using digital fundus images has become a reality with AI assistance [26 27]. However, the sensitivity was limited to a moderate level, because some peripheral CMVR lesions could be missed in digital fundus images. Compared with traditional single field or mosaic fundus images, UWF fundus images, with a 200-degree field of the retina, showed overwhelming advantages for capturing the whole CMVR lesions [12 28].UWF fundus image has also shown significant potential in the automatic diagnosis of retinal diseases [26,27]. However, the role of DL approaches in detecting CMVR from UWF fundus images has yet to be determined.

With an urgent need for routine CMVR screening for AIDS patients and the great success of DL in clinical medicine, the current research aimed to develop a novel deep learning system for automated detection of CMVR with UWF fundus images alone to determine its possible use for AIDS-related CMVR screening and classification. To address this, we selected suitable neural network architecture to train and validate deep learning models using retrospectively collected UWF fundus images. Additionally, we also verified its performance with prospective validation datasets and external validation datasets from different clinical settings.

1.1. Related researches

Some researchers have made progress in screening CMVR in a telemedicine and AI scenario. Table 1 summarizes the research, including algorithms, models, sample size, image modality, etc. A detailed comparison between these researches and the present study is completed in the *Discussion* section.

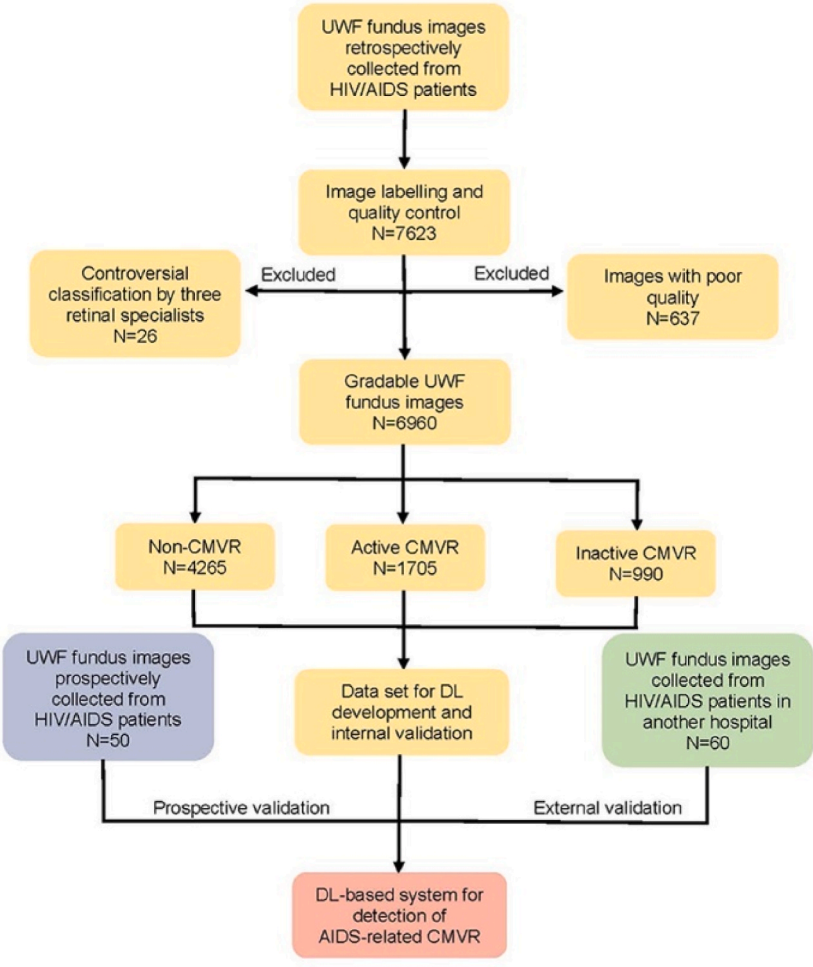

Fig. 1. The flow chart of data selection.

2. Materials and methods

2.1. Study design and participants

Current research was performed in Beijing Youan Hospital (Beijing, China) and Beijing Tongren Hospital (Beijing, China). In the first step, UWF images from HIV/AIDS patients attained using an OPTOS non-mydriatic camera (OPTOS® Daytona) were retrospectively collected from Beijing Youan Hospital between September 5, 2017 and October 31, 2020. The whole dataset was randomly split into two independent datasets with five-fold cross-validation: training and internal validation datasets [30]. The flow chart is shown in Fig. 1. If multiple images were obtained from the same eye, those images were included either in the training dataset or the internal validation dataset.

In the second step, we validated the performance of the DL system. Another group of HIV/AIDS patients was retrospectively collected from Beijing Tongren Hospital between June 1, 2018 and November 30, 2020 as an external dataset. Their UWF fundus images were attained using another OPTOS camera of a different type (OPTOS® 200Tx).

In the last stage, to further evaluate the applicability of the DL system, the UWF fundus images from HIV/AIDS patients who received OPTOS camera (OPTOS® Daytona) evaluation from Beijing Youan Hospital were collected as a prospective dataset (from April 1, 2021 to May 1, 2021).

In real clinical scenes, stable CMVR means treated CMVR, and its severity is located between normal and active CMVR. Moreover, the sample number of stable CMVR is small. Therefore, we designed three binary classification problems (Active CMVR versus non-CMVR, Active CMVR versus non-CMVR and stable CMVR, and Active CMVR and stable CMVR versus non-CMVR).

This research was conducted following the Declaration of Helsinki. Both the Ethics Committee of Beijing YouAn Hospital (LL-2018-150-K) and the Ethics Committee of Beijing Tongren Hospital (TRECKY2018-056) approved this research. Written informed consent was obtained from each subject. This trial is registered with ClinicalTrials.gov (NCT04831333).

2.2. Image labeling

Two experienced retinal specialists with more than 5 years of clinical experience in reading all UWF images independently and classified them into three groups: active CMVR, inactive CMVR, and non-CMVR. Any disagreement between the two human graders was further diagnosed by another senior retinal specialist. The UWF images of CMVR included various presentations: hemorrhagic necrotizing lesion, granular lesion, frosted branch angiitis, and optic neuropathy lesion [12]. Active CMVR and inactive CMVR were differentiated according to clinical evaluation and the opacity of the borders of the CMVR lesion [31]: active CMVR lesion was defined as obvious opacity (mild, moderate, severe, very severe), whereas inactive CMVR lesion was defined as a lack of opacity or questionable/equivocal activity. The non-CMVR images included normal retina and other retinopathies such as HIV-related microvascular retinopathy, diabetic retinopathy, retinal detachment, and vitreous hemorrhage (Fig. 2). These image labels were considered as reference standards for training and validation in this study. During image labeling, images were excluded if human graders did not give a consensus.

2.3. Image preprocessing and quality control

To improve the DL analysis, we resized the images to a unified resolution of 512 × 512 before developing the algorithm. In the control quality process, we filtered out unqualified images based on several criteria (the readable region ratio, illumination, blurriness, and image contents). The pixel intensity of the selected images was normalized from (0, 255) to (0, 1).

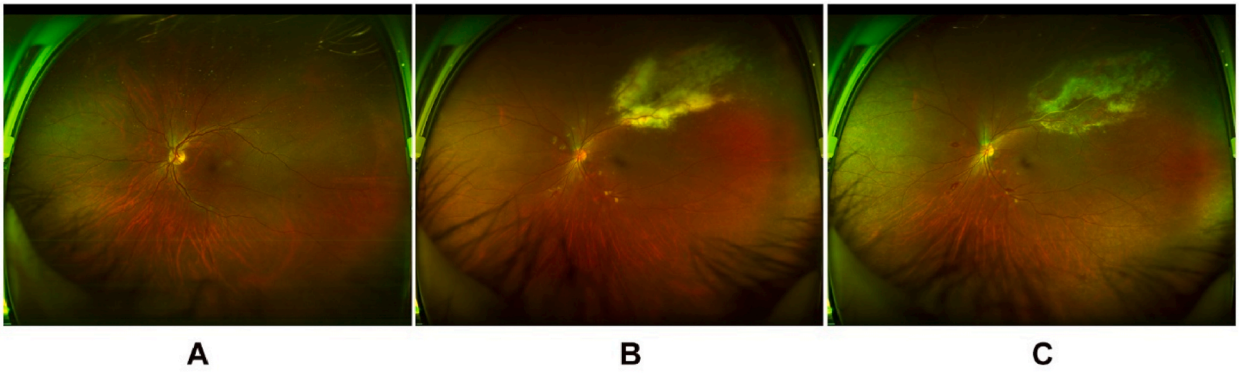

Fig. 2. Image examples of non-CMVR (a), active CMVR (b), and inactive CMVR (c).

2.4. Algorithm development

We applied a convolutional neural network to automatically detect CMVR. We first compared the performance of some architectures including ResNet-50 [32], ResNet-101 [33,34], InceptionV3 [35], InceptionV4, and InceptionResnetV2 [36]. InceptionResnetV2 [37], which achieved the best performance, was finally chosen to complete the task. Three models were separately trained to differentiate the following binary classification tasks: (1) active CMVR versus non-CMVR, (2) active CMVR versus non-CMVR and inactive CMVR and (3) active CMVR and inactive CMVR versus non-CMVR (Fig. 3). We established these three models for the better application in various clinical situations. We adopted subject independently [38,39] five-fold cross validation [40–42] to fairly test the performance of the models and selected the optimal one, at the same time, convolutional neural network (CNN) architectures were fine-tuned with the pre-trained models constructed with ImageNet dataset [43]. Furthermore, cross-validation is carried out in a subject-independent manner, namely, the images from one patient will not be split into training and validation datasets. To further test the performance of the DL models, we then used external validation and prospective validation datasets. All models were developed with TensorFlow 1.10.0 and Keras 2.2.4 [36] on a server with four TITAN XP GPUs. Because the dataset is imbalanced, we adopted class weights to avoid the biased towards the majority class [44].

2.5. Visualisation heat map

We used Grad-CAM [45] to study whether DL models were able to detect the lesions in UWF fundus images. The results were presented as heat maps, which showed some pixels (red) as the most important clues for the classification task.

2.6. Comparison between human and DL

Two retinal ophthalmologists: a senior and a junior were required to independently evaluate the UWF fundus images in the prospective validation dataset. We compared the performance of these trained human ophthalmologists with the DL system.

2.7. Statistical analyses

All statistical analyses were performed using Python 3.7.3 (Wilmington, DE, USA) and MATLAB R2016a (https://www.mathworks.com/). We used the accuracy, sensitivity, specificity, and receiver operating characteristic (ROC) curve to assess the performance of the DL model. The area under the ROC curve (AUROC) with a 95 % confidence interval (CI) was calculated [46], in an internal cross validation dataset, point estimation was used to figure out the corresponding confidence interval [47]. Whereas in prospective and external validation, N-out-of-N Bootstrapping with 1000 replicates was used to estimate 95 % confidence intervals (95 % CI).

3. Results

Totally 6960 gradable UWF fundus images of 862 AIDS patients were retrospectively gathered for the training, tuning, and internal validation of the DL system (Table 2). Patients in this study were predominantly male (93.0 %), with a mean age of 38.8 ± 11.5 years. Most images were labeled as non-CMVR (61.3 %), and the percentages for active CMVR/inactive CMVR were 24.5 %/14.2 %. Sixty UWF images from 30 AIDS patients and 50 UWF images from 25 AIDS patients were collected as the external validation dataset and prospective validation dataset, respectively. Similar age, sex distribution, and percentages of non-CMVR, active CMVR, and inactive

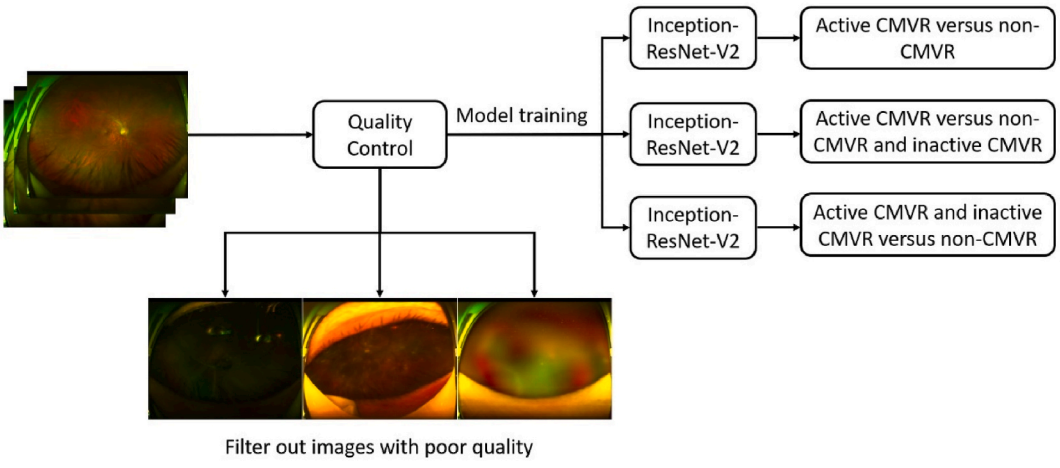

Fig. 3. Overview of a deep convolutional neural network–based model training pipeline to automatically identify active CMVR, inactive CMVR, and non-CMVR from ultra-wide-field fundus images.

Table 2
Demographics and characteristics of the datasets.

Characteristic	Beijing Youan Hospital		Beijing Tongren Hospital
	Development dataset and internal validation dataset	Prospective validation dataset	External validation dataset
Total number of images	6979	50	60
Total number of gradable images	6960	50	60
Number of individuals	862	25	30
Number of men (%)	802 (93.0)	22 (88.0)	25 (83.3)
Age (mean ± SD, y)	38.8 ± 11.5	42.8 ± 14.7	36.6 ± 13.2
Non-CMVR[a]	4265 (61.3)	27 (54.0)	32 (53.3)
Active CMVR[a]	1705 (24.5)	20 (40.0)	26 (43.3)
Inactive CMVR[a]	990 (14.2)	3 (6.0)	2 (3.3)

[a] Data are presented as the number of images (percentage in total number of gradable, %). SD, standard deviation; CMVR, cytomegaloviral retinitis.

CMVR were recognized in the different datasets.

Table 3 displays the performance of the DL models to detect CMVR. All three models reached an average accuracy of greater than 0.88 in the internal cross-validation. The average sensitivity and specificity were greater than 0.77 and 0.92, respectively, and the mean AUROCs were greater than 0.93 (Fig. 4). ROC curves are from the best models whose AUROC values are maximum. For the external validation dataset, both the accuracy and sensitivity surpassed 0.87 in the three tasks. The specificity and AUROCs surpassed 0.81 and 0.93, respectively, in the three tasks. For the prospective validation dataset, the accuracy, sensitivity, specificity, and AUROC were greater than 0.93 in the first task. In the second task, except for the sensitivity being 0.8333, the other evaluation metrics were greater than 0.90. For the third task, all metrics were higher than 0.92.

When comparing the performance between human ophthalmologists and the DL system, we found that the senior retinal ophthalmologist showed better average accuracy, sensitivity, and specificity than the junior retinal ophthalmologist did in all three tasks (Supplementary Table 1). In general, the performance of the DL system is better than that of the junior retinal ophthalmologist and reached a level similar to that of the senior retinal ophthalmologist (Fig. 4).

The heat maps showed that regardless of whether the lesions were located at the peripheral retina, posterior retina, or the whole retina, DL successfully highlighted the locations of the lesions (true-positive findings; Fig. 5).

4. Discussion

To the best of our knowledge, this is the first DL system to screen AIDS-related CMVR from UWF fundus image. In this study, we developed, internally validated, externally validated, and prospectively validated a novel UWF fundus image-based DL system to screen CMVR in HIV/AIDS patients. This DL system showed consistently great performance for differentiating between eyes with active CMVR and eyes with non-CMVR. In addition, our DL system also had good performance with the presence of inactive CMVR, thus allowing screening in clinical settings.

Early detection of CMVR is crucial to curb AIDS-related blindness and mortality. Patients with AIDS who have CMVR have a high risk of mortality, which could be reduced by the use of systemic anti-cytomegalovirus therapy [48]. Kingkosol and colleagues proposed an artificial neural network (ANN) for automated CMVR screening in immunodeficient patients using digital fundus images [28].

Table 3
Performance of the algorithms in different validation datasets.

Classification	Dataset	Accuracy (95 % CI)	Sensitivity (95 % CI)	Specificity (95 % CI)	AUROC (95 % CI)
Active CMVR versus non-CMVR	Internal cross-validation[a]	0.923 (0.908, 0.938)	0.8015 (0.722, 0.881)	0.9704 (0.952, 0.989)	0.9454 (0.929, 0.962)
	External validation	0.879 (0.794, 0.918)	0.9615 (0.869, 0.997)	0.8125 (0.733, 0.854)	0.9636 (0.870, 0.999)
	Prospective validation	0.957 (0.851, 0.995)	1.0000 (0.889, 1.000)	0.9310 (0.827, 0.970)	0.9676 (0.860, 1.000)
Active CMVR versus non-CMVR and inactive CMVR	Internal cross-validation[a]	0.902 (0.857, 0.948)	0.7759 (0.659, 0.893)	0.9428 (0.848, 1.000)	0.9333 (0.900, 0.967)
	External validation	0.900 (0.814, 0.938)	0.9615 (0.871, 0.997)	0.8529 (0.771, 0.892)	0.9819 (0.889, 1.000)
	Prospective validation	0.900 (0.803, 0.940)	0.8333 (0.743, 0.876)	0.9375 (0.837, 0.976)	0.9058 (0.809, 0.945)
Active CMVR and inactive CMVR versus non-CMVR	Internal cross-validation[a]	0.884 (0.851, 0.917)	0.8225 (0.639, 1.000)	0.9234 (0.843, 1.000)	0.9393 (0.895, 0.983)
	External validation	0.900 (0.814, 0.938)	0.9286 (0.841, 0.965)	0.8750 (0.792, 0.913)	0.9686 (0.877, 1.000)
	Prospective validation	0.940 (0.839, 0.978)	0.9524 (0.851, 0.990)	0.9310 (0.831, 0.969)	0.9294 (0.830, 0.968)

data is presented as the mean value of the AUROC in five-fold internal cross-validation. CMVR, cytomegaloviral retinitis; CI, confidence interval.

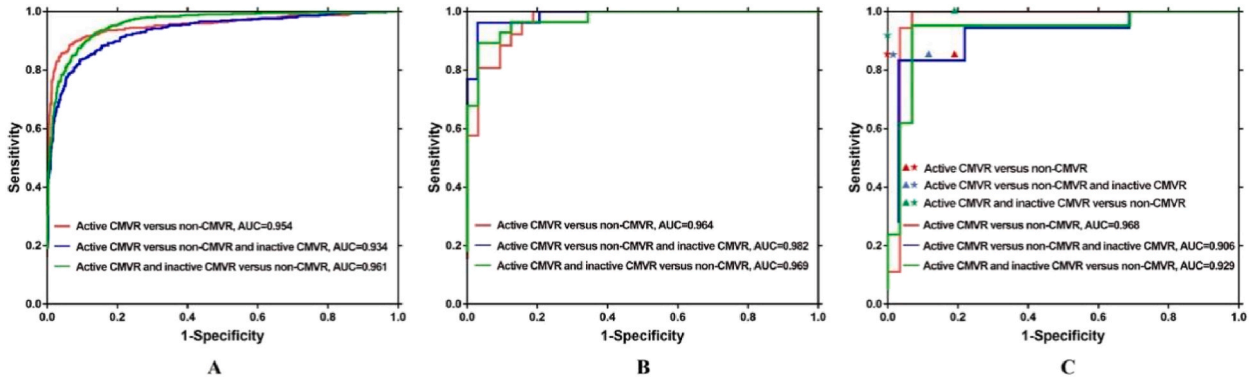

Fig. 4. Receiver-operating characteristic curves illustrate the performance of the algorithms and human ophthalmologists in internal cross-validation (a), external validation (b), and prospective validation (c). Triangle: junior retinal ophthalmologist; pentagram: senior retinal ophthalmologist.

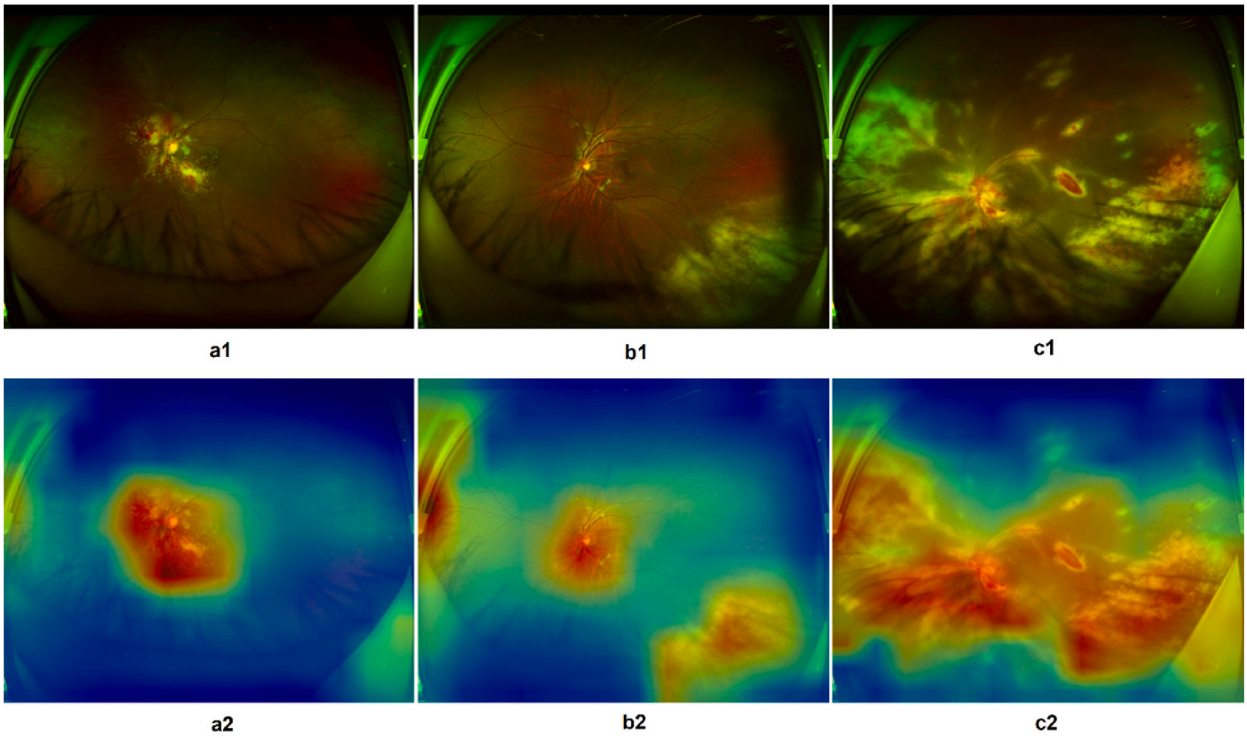

Fig. 5. Ultra-wide-field fundus images and corresponding heat maps showing typical true-positive cases. Lesions shown in a1, b1, and c1 correspond to the highlighted regions displayed in heat maps a2, b2, and c2, respectively.

Srisuriyajan and colleagues proposed a CNN for automated CMVR screening using digital fundus images [29]. Ong et al. developed a multi-task learning model to detect necrotizing viral retinitis, including CMVR from common blood and serology tests (varicella-zoster virus immunoglobulin M (IgM), CMV IgM, and lymphocyte count). The related literature has been summarized in Table 1. Although their results were promising and provided proof-of-concept data on using AI to automate CMVR screening, their findings were based on a small sample. In addition, the sensitivity was limited to a moderate level, because these retinal fundus images were captured by a traditional digital fundus camera with a 45-degree retinal view, which might miss the peripheral necrotic retinitis. As compared with traditional fundus montage photography, the UWF fundus image in this study, with a 200-degree field of the retina, showed overwhelming advantages for capturing the whole CMVR lesions [49]. By contrast, our DL system was developed with 6960 UWF fundus images from 862 AIDS patients, with 24.5 % of eyes with active CMVR, thus improving the efficiency of our DL system.

To increase applicability, we intentionally included UWF fundus images obtained by different OPTOS cameras (OPTOS® 200Tx and Daytona) from different clinical centers. Meanwhile, we also intentionally included eyes with inactive CMVR. Because studies

have shown some HIV/AIDS patients could present with healed scars consistent with CMVR [50,51]. Of note, our DL system has good robustness in differentiating active CMVR from non-CMVR and inactive CMVR. These findings suggest that active CMVR has remarkable UWF image features that can be easily distinguished from other eye diseases.

HIV/AIDS-related discrimination and stigma are identified barriers to the control of the AIDS epidemic and are common among healthcare providers in various countries [52,53]. A more comprehensive health system for HIV patients could help to address challenges. New strategies have been promoted, including the integration of both HIV and non-HIV medical services [54]. Our proposed UWF fundus image-based DL system provides a proof-of-concept solution to address the current gap in AIDS-related CMVR screening, Firstly, this DL system-based CMVR diagnosis can be conducted without the assistance of retinal specialists. The identified patients can then be referred to inpatients with subsequent systemic anti-CMV treatment and other opportunistic infection screening because CMVR is an important sign of the AIDS stage. Secondly, CMV-DNA tests of ocular specimens [55] or manual observation of the opacity of CMVR lesion borders [31] were used to monitor the efficacy of anti-CMV treatment. This DL system could also be implemented as a cost-effective and noninvasive tool for monitoring CMVR via discerning active CMVR from inactive CMVR. It can improve the patient's ability to follow-up. Thirdly, with advances in DL technology and the increasing popularity of non-mydriatic UWF fundus cameras, a future CMVR self-screening program using our DL system holds promise and could also be high-demanding, such as with HIV self-testing in China [56].

Strengths of this study include a large clinical HIV/AIDS sample, with datasets from different clinical centers and different fundus cameras. Furthermore, this DL system was based on a non-mydriatic, noninvasive, and 200-degree field fundus image with reasonably high AUROC, sensitivity, and specificity. In general, the DL system has reached a similar diagnostic level to that of a senior retinal ophthalmologist. The heat maps also prove that the system was able to precisely locate the lesions, which is similar to the working style of the human brain. At the same time, we have selected a suitable neural network architecture for UWF fundus images which covers more area than conventional fundus images.

Several limitations of current research should be discussed. Firstly, our dataset cannot cover all populations from multiple ethnic and regions. Although our study included a considerable number of HIV/AIDS patients, we did not involve non-HIV-related CMVR because of its great variety and rarity. CMVR shows similar clinical features in patients both with and without HIV, including the rate of foveal involvement, retinal detachment, involved zone, mortality of CMVR, and types of retinitis (fulminant/indolent) [57,58]. Future investigations should focus on the use of our DL system in CMVR screening in various non-HIV populations, which may have similar results to those obtained in our study. Secondly, a few eyes with CMVR might present complications, such as cataracts or vitreous hemorrhage/inflammation [1], which could be excluded from the present dataset. However, such cases were also a challenge for retinal specialists, and could not necessarily weaken the present results. In addition, various commercial fundus cameras, such as Zeiss Clarus® systems, are also widely used. These cameras have properties that are different from those of the OPTOS system [59]. Whether our results will apply to other UWF cameras or real-world settings deserves further investigation.

5. Conclusions

In conclusion, we developed, internally validated, externally validated, and prospectively validated a UWF fundus image-based DL system to screen CMVR in HIV/AIDS patients. Our study provides a unique and novel model that could be used in clinical settings, especially in the absence of ophthalmic resources. Further clinical investigation of this DL system across diverse populations, clinical settings, or different retinal cameras in the real world will be required. Some comorbidity should be included to construct a real clinical circumstance that could improve the robustness of the DL system. Additionally, multi-modality data could be integrated to build a comprehensive diagnostic model for CMVR.

Ethics approval and consent to participate

Both the Ethics Committees of Beijing YouAn Hospital (LL-2018-150-K) and Beijing Tongren Hospital (TRECKY2018-056) approved the study. Written informed consent was obtained from each subject.

Consent for publication

N/A.

Availability of data and materials

The datasets and code used in this work and the full study protocol are available from the corresponding author upon reasonable request.

Funding

The work was supported by Scientific Research Project of Beijing Youan Hospital, CCMU, 2018, China (grant YNKTQN20180201); the National Natural Science Foundation of China, China (grant 82,220,108,017, grant 82,141,128); The Capital Health Research and Development of Special, China (grant 2020-1-2052); Science & Technology Project of Beijing Municipal Science & Technology Commission, China (grant Z201100005520045, grant Z181100001818003); Sanming Project of Medicine in Shenzhen, China (grant

SZSM202311018).

Ethical approval

Both the Ethics Committee of Beijing YouAn Hospital (LL-2018-150-K) and the Ethics Committee of Beijing Tongren Hospital (TRECKY2018-056) approved this research.

CRediT authorship contribution statement

Kuifang Du: Writing – review & editing, Writing – original draft, Formal analysis, Data curation, Conceptualization. **Li Dong:** Writing – review & editing, Resources, Data curation, Conceptualization. **Kai Zhang:** Writing – review & editing, Software, Methodology, Investigation, Formal analysis. **Meilin Guan:** Investigation, Data curation. **Chao Chen:** Visualization, Project administration, Data curation. **Lianyong Xie:** Validation, Data curation. **Wenjun Kong:** Supervision, Investigation. **Heyan Li:** Validation, Software. **Ruiheng Zhang:** Supervision, Project administration. **Wenda Zhou:** Investigation, Data curation. **Haotian Wu:** Software, Investigation. **Hongwei Dong:** Writing – review & editing, Supervision, Resources. **Wenbin Wei:** Writing – review & editing, Supervision, Funding acquisition, Data curation, Conceptualization.

Declaration of competing interest

The authors declare that they have no known competing financial interests or personal relationships that could have appeared to influence the work reported in this paper.

Acknowledgments

N/A.

Appendix A. Supplementary data

Supplementary data to this article can be found online at https://doi.org/10.1016/j.heliyon.2024.e30881.

References

[1] M. Munro, T. Yadavalli, C. Fonteh, S. Arfeen, A.-M. Lobo-Chan, Cytomegalovirus retinitis in HIV and non-HIV individuals, Microorganisms 8 (1) (2020) 55.
[2] G. Li, Y. Jiang, L. Zhang, HIV Upsurge in China's Students, American Association for the Advancement of Science, 2019.
[3] D. Heiden, P. Saranchuk, N. Tun, et al., We urge WHO to act on cytomegalovirus retinitis, Lancet Global Health 2 (2) (2014) e76–e77.
[4] N. Ford, Z. Shubber, P. Saranchuk, et al., Burden of HIV-related cytomegalovirus retinitis in resource-limited settings: a systematic review, Clin. Infect. Dis. 57 (9) (2013) 1351–1361.
[5] Cytomegalovirus retinitis screening and treatment in human immunodeficiency virus patients in Malawi: a feasibility study, Open Forum Infectious Diseases, Oxford University Press US, 2019.
[6] N. Morlet, S. Young, R. Dean, J. Gold, Ophthalmological screening for CMV retinits in HIV infection, Lancet (British edition) 340 (8812) (1992).
[7] T. Nishijima, S. Yashiro, K. Teruya, et al., Routine eye screening by an ophthalmologist is clinically useful for HIV-1-infected patients with CD4 count less than 200/μL, PLoS One 10 (9) (2015) e0136747.
[8] S.H. Vermund, HIV/AIDS trends in China, Lancet Infect. Dis. 13 (11) (2013) 912–914.
[9] M. Yen, S. Ausayakhun, J. Chen, et al., Telemedicine diagnosis of cytomegalovirus retinitis by nonophthalmologists, JAMA Ophthalmology 132 (9) (2014) 1052–1058, https://doi.org/10.1001/jamaophthalmol.2014.1108 [published Online First: Epub Date]|.
[10] J.M. Shah, S.W. Leo, J.C. Pan, et al., Telemedicine screening for cytomegalovirus retinitis using digital fundus photography, Telemedicine and e-Health 19 (8) (2013) 627–631, https://doi.org/10.1089/tmj.2012.0233 [published Online First: Epub Date]|.
[11] C. Jirawison, M. Yen, P. Leenasirimakul, et al., Telemedicine screening for cytomegalovirus retinitis at the point of care for human immunodeficiency virus infection, JAMA ophthalmology 133 (2) (2015) 198–205.
[12] K.-F. Du, C. Chen, X.-J. Huang, et al., Utility of ultra-wide-field imaging for screening of AIDS-related cytomegalovirus retinitis, Ophthalmologica 244 (4) (2021) 334–338.
[13] KT-i Ong, T. Kwon, H. Jang, et al., Multitask deep learning for Joint detection of necrotizing viral and noninfectious retinitis from common blood and serology test data, 5-5, Investigative Ophthalmology & Visual Science 65 (2) (2024), https://doi.org/10.1167/iovs.65.2.5 [published Online First: Epub Date]|.
[14] K.-F. Du, X.-J. Huang, C. Chen, et al., High blood cytomegalovirus Load suggests cytomegalovirus retinitis in HIV/AIDS patients: a cross-Sectional study, Ocul. Immunol. Inflamm. 30 (7–8) (2022) 1559–1563, https://doi.org/10.1080/09273948.2021.1905857 [published Online First: Epub Date]|.
[15] G. Litjens, T. Kooi, B.E. Bejnordi, et al., A survey on deep learning in medical image analysis, Med. Image Anal. 42 (2017) 60–88.
[16] C.J. Haug, J.M. Drazen, Artificial intelligence and Machine learning in clinical medicine, New England Journal of Medicine 2023 388 (13) (2023) 1201–1208, https://doi.org/10.1056/NEJMra2302038 [published Online First: Epub Date]|.
[17] V. Biousse, N.J. Newman, R.P. Najjar, et al., Optic disc classification by deep learning versus expert neuro-ophthalmologists, Ann. Neurol. 88 (4) (2020) 785–795.
[18] D.S. Kermany, M. Goldbaum, W. Cai, et al., Identifying medical diagnoses and treatable diseases by image-based deep learning, Cell 172 (5) (2018) 1122–1131. e9.
[19] Z. Li, Y. He, S. Keel, W. Meng, R.T. Chang, M. He, Efficacy of a deep learning system for detecting glaucomatous optic neuropathy based on color fundus photographs, Ophthalmology 125 (8) (2018) 1199–1206.
[20] D.S.W. Ting, C.Y.-L. Cheung, G. Lim, et al., Development and validation of a deep learning system for diabetic retinopathy and related eye diseases using retinal images from multiethnic populations with diabetes, JAMA 318 (22) (2017) 2211–2223.

[21] V. Gulshan, L. Peng, M. Coram, et al., Development and validation of a deep learning algorithm for detection of diabetic retinopathy in retinal fundus photographs, JAMA 316 (22) (2016) 2402–2410.
[22] W. Li, Y. Yang, K. Zhang, et al., Dense anatomical annotation of slit-lamp images improves the performance of deep learning for the diagnosis of ophthalmic disorders, Nat. Biomed. Eng. 4 (8) (2020) 767–777.
[23] Z. Li, C. Guo, D. Nie, et al., A deep learning system for identifying lattice degeneration and retinal breaks using ultra-widefield fundus images, Ann. Transl. Med. 7 (22) (2019).
[24] D.S. Ting, L. Peng, A.V. Varadarajan, et al., Deep learning in ophthalmology: the technical and clinical considerations, Prog. Retin. Eye Res. 72 (2019) 100759.
[25] L. Wang, K. Zhang, X. Liu, et al., Comparative analysis of image classification methods for automatic diagnosis of ophthalmic images, Sci. Rep. 7 (1) (2017) 1–11.
[26] D. Nagasato, H. Tabuchi, H. Masumoto, et al., Prediction of age and brachial-ankle pulse-wave velocity using ultra-wide-field pseudo-color images by deep learning, Sci. Rep. 10 (1) (2020) 1–9.
[27] Zhang W., juan Zhao X., Chen Y., Zhong J., Yi Z., DeepUWF: an automated ultra-wide-field fundus screening system via deep learning, IEEE Journal of Biomedical and Health Informatics 25 (8) (2021) 2988-2996.
[28] Automated Cytomegalovirus Retinitis Screening in Fundus Images, 2020 42nd Annual International Conference of the IEEE Engineering in Medicine & Biology Society (EMBC), IEEE, 2020.
[29] P. Srisuriyajan, N. Cheewaruangroj, P. Polpinit, W. Laovirojjanakul, Cytomegalovirus RETINITIS screening using machine learning technology, Retina 42 (9) (2022).
[30] K. Zhang, X. Liu, J. Jiang, et al., Prediction of postoperative complications of pediatric cataract patients using data mining, J. Transl. Med. 17 (1) (2019) 1–10.
[31] G.N. Holland, M.L. Van Natta, D.T. Goldenberg, et al., Relationship between opacity of cytomegalovirus retinitis lesion borders and severity of immunodeficiency among people with AIDS, Invest. Ophthalmol. Vis. Sci. 60 (6) (2019) 1853–1862.
[32] Q. Pan, K. Zhang, L. He, et al., Automatically diagnosing disk bulge and disk herniation with lumbar magnetic resonance images by using deep convolutional neural networks: method development study, JMIR medical informatics 9 (5) (2021) e14755.
[33] K. Zhang, X. Li, L. He, et al., A human-in-the-loop deep learning paradigm for synergic visual evaluation in children, Neural Network. 122 (2020) 163–173.
[34] J. Yang, K. Zhang, H. Fan, et al., Development and validation of deep learning algorithms for scoliosis screening using back images, Commun. Biol. 2 (1) (2019) 1–8.
[35] K. Zhang, X. Liu, F. Liu, et al., An interpretable and expandable deep learning diagnostic system for multiple ocular diseases: qualitative study, J. Med. Internet Res. 20 (11) (2018) e11144.
[36] Z. Li, C. Guo, D. Nie, et al., Deep learning for detecting retinal detachment and discerning macular status using ultra-widefield fundus images, Commun. Biol. 3 (1) (2020) 1–10.
[37] W.-D. Zhou, L. Dong, K. Zhang, et al., Deep learning for automatic detection of recurrent retinal detachment after surgery using ultra-widefield fundus images: a single-center study, n/a(n/a), Advanced Intelligent Systems (2022) 2200067, https://doi.org/10.1002/aisy.202200067 [published Online First: Epub Date]|.
[38] K. Zhang, Y. Zhang, Y. Ding, et al., Anatomical sites identification in both ordinary and capsule gastroduodenoscopy via deep learning, Biomed. Signal Process Control 90 (2024) 105911, https://doi.org/10.1016/j.bspc.2023.105911 [published Online First: Epub Date]|.
[39] Y. Zhang, K. Zhang, Y. Ding, et al., Deep transfer learning from ordinary to capsule esophagogastroduodenoscopy for image quality controlling, n/a(n/a), Engineering Reports (2023) e12776, https://doi.org/10.1002/eng2.12776 [published Online First: Epub Date]|.
[40] X. Zhang, K. Zhang, D. Lin, et al., Artificial intelligence deciphers codes for color and odor perceptions based on large-scale chemoinformatic data, GigaScience 9 (2) (2020) giaa011.
[41] Y. Zhang, F. Li, F. Yuan, et al., Diagnosing chronic atrophic gastritis by gastroscopy using artificial intelligence, Dig. Liver Dis. 52 (5) (2020) 566–572.
[42] S. Hui, L. Dong, K. Zhang, et al., Noninvasive identification of Benign and malignant eyelid tumors using clinical images via deep learning system, Journal of Big Data 9 (1) (2022) 84, https://doi.org/10.1186/s40537-022-00634-y [published Online First: Epub Date]|.
[43] A. Imagenet, large-scale hierarchical image database. 2009 IEEE Conference on Computer Vision and Pattern Recognition, Ieee, 2009.
[44] R. Zhang, L. Dong, R. Li, et al., Automatic retinoblastoma screening and surveillance using deep learning, Br. J. Cancer 129 (3) (2023) 466–474, https://doi.org/10.1038/s41416-023-02320-z [published Online First: Epub Date]|.
[45] Grad-cam: visual explanations from deep networks via gradient-based localization, Proceedings of the IEEE International Conference on Computer Vision, 2017.
[46] H. Zhang, Y. Liu, K. Zhang, et al., Validation of the relationship between iris color and uveal melanoma using artificial intelligence with multiple paths in a large Chinese population, Front. Cell Dev. Biol. 9 (2021).
[47] Variability in Primary Care Physician Attitudes Toward Medicaid Work Requirement Exemption Requests Made by Patients With Depression, in: JAMA Health Forum, American Medical Association, 2021.
[48] J.H. Kempen, D.A. Jabs, L.A. Wilson, J.P. Dunn, S.K. West, J. Tonascia, Mortality risk for patients with cytomegalovirus retinitis and acquired immune deficiency syndrome, Clin. Infect. Dis. 37 (10) (2003) 1365–1373.
[49] S.S. Mudvari, V.V. Virasch, R.M. Singa, M.W. MacCumber, Ultra-wide–field imaging for cytomegalovirus retinitis, Ophthalmic Surgery, Lasers and Imaging Retina 41 (3) (2010) 311–315.
[50] B.C. Fishburne, A.A. Mitrani, J.L. Davis, Cytomegalovirus retinitis after cardiac transplantation, Am. J. Ophthalmol. 125 (1) (1998) 104–106, https://doi.org/10.1016/S0002-9394(99)80245-1 [published Online First: Epub Date]|.
[51] M.-K. Song, S.P. Azen, A. Buley, et al., Effect of anti-cytomegalovirus therapy on the incidence of immune recovery uveitis in AIDS patients with healed cytomegalovirus retinitis, Am. J. Ophthalmol. 136 (4) (2003) 696–702, https://doi.org/10.1016/S0002-9394(03)00335-0 [published Online First: Epub Date]|.
[52] X. Dong, J. Yang, L. Peng, et al., HIV-related stigma and discrimination amongst healthcare providers in Guangzhou, China, BMC Publ. Health 18 (1) (2018) 1–10.
[53] A. Geter, A.R. Herron, M.Y. Sutton, HIV-related stigma by healthcare providers in the United States: a systematic review, AIDS patient care and STDs 32 (10) (2018) 418–424.
[54] K. Safreed-Harmon, J. Anderson, N. Azzopardi-Muscat, et al., Reorienting health systems to care for people with HIV beyond viral suppression, The Lancet HIV 6 (12) (2019) e869–e877.
[55] I.L. Smith, J.C. Macdonald, W.R. Freeman, A.M. Shapiro, S.A. Spector, Cytomegalovirus (CMV) retinitis activity is accurately reflected by the presence and level of CMV DNA in aqueous humor and vitreous, J. Infect. Dis. 179 (5) (1999) 1249–1253.
[56] W. Tang, D. Wu, Opportunities and challenges for HIV self-testing in China, The lancet HIV 5 (11) (2018) e611–e612.
[57] M. Ho, A. Invernizzi, S. Zagora, et al., Presenting features, treatment and clinical outcomes of cytomegalovirus retinitis: non-HIV patients vs HIV patients, Ocul. Immunol. Inflamm. (2019).
[58] D.Y. Kim, J. Jo, S.G. Joe, J.-G. Kim, Y.H. Yoon, J.Y. Lee, Comparison of visual prognosis and clinical features of cytomegalovirus retinitis in HIV and non-HIV patients, Retina 37 (2) (2017) 376–381.
[59] Y. Matsui, A. Ichio, A. Sugawara, et al., Comparisons of effective fields of two ultra-widefield ophthalmoscopes, Optos 200Tx and Clarus 500, BioMed Res. Int. 2019 (2019).